

## Hartree-Fock approximation for the quasiparticle properties of the coupled electron-phonon system in quantum-well wires in the presence of a magnetic field

L. Wendler

*Anna-Siemsen-Straße 66, D-07745 Jena, Germany*

(Received 9 July 1997; revised manuscript received 6 November 1997)

A theory is presented that allows the calculation of the quasiparticle properties of lower-dimensional semiconductor nanostructures in the framework of a diagrammatic approach of many-particle Green's-function technique in subband space. We apply this theory to consider the interaction of quasi-one-dimensional electrons and longitudinal-optical (LO) phonons in the presence of a quantizing magnetic field. An expression for the electron matrix self-energy in subband space has been derived in the Hartree-Fock approximation of Feynman-Dyson perturbation theory. Numerical results for the energy-momentum relation and the effective mass have been obtained for the magnetopolaron states in quantum-well wires. It is shown that the Tamm-Dancoff approximation and its on-mass-shell version fail for the calculation of the renormalization of the excited subband energies in quantum-well wires with strong lateral confining potentials even for vanishing magnetic field and polaron momentum. In this case only the Hartree-Fock approximation gives the correct quasiparticle properties. [S0163-1829(98)02315-7]

Quasi-one-dimensional (Q1D) electron systems, such as occur in semiconductor quantum-well wires (QWW's), are particularly interesting systems to study interaction processes. Here, we study the electron-phonon interaction in the presence of a quantizing magnetic field and investigate the quasiparticle properties of the coupled electron-phonon system.

Most of the currently studied QWW's are based on III-V compound semiconductors that are weakly polar. Electrons moving through such samples polarize their surroundings and couple to this self-induced polarization field, which is connected with lattice vibrations in optical modes. Only the long-wavelength optical phonons have large electric dipole moments and, thus, only these phonons take part on the electron-phonon interaction. The electron-phonon interaction modifies the electronic properties by (i) forming quasiparticle states, the Q1D magnetopolarons, consisting of an electron and its surrounding phonon cloud and (ii) forming a phonon continuum for energies above a threshold energy. In 3D bulk semiconductors (see, e.g., Refs. 1 and 2), strict 2D and Q2D semiconductor quantum-well systems (see, e.g., Refs. 3–11) polarons and magnetopolarons are intensively investigated. It has been shown<sup>12</sup> that the polaronic effects increase as the dimensionality of the structure is reduced. Q1D polarons<sup>13–16</sup> and Q1D magnetopolarons<sup>17</sup> calculated in Rayleigh-Schrödinger, Wigner-Brillouin, and improved Wigner-Brillouin perturbation theory show interesting features. So, for Q1D magnetopolarons it depends on the ratio of the confinement energy to the phonon energy, whether for the first excited subband a resonant magnetopolaron case near the lower boundary of the one-phonon continuum is possible or not. Further, the Q1D cyclotron mass shows a minimum for a finite value of the magnetic field.<sup>17</sup>

The aim of the present paper is to develop a more complete theory of the quasiparticle properties, i.e., of the energy-momentum relation, damping, renormalization factor, and effective mass, for interacting electrons in lower-dimensional nanostructures using many-particle Green's-

function technique. Applying this theory to the Q1D magnetopolaron problem, we calculate an expression for the electron matrix self-energy in the subband space in the framework of the Hartree-Fock approximation of the Feynman-Dyson perturbation theory, i.e., in a diagrammatic approach.

We study the QWW by a model in which the electrons are confined in a zero-thickness  $x$ - $y$  plane along the  $z$  direction at  $z=0$ . In the  $y$  direction the electron motion is assumed to be quantum confined by a parabolic potential,  $V(y) = m_e \Omega^2 y^2 / 2$ , where  $m_e$  is the effective conduction-band-edge mass and  $\Omega$  is the confining frequency. Choosing the Landau gauge  $\mathbf{A}(\mathbf{x}) = (-yB, 0, 0)$  for the vector potential of the externally applied static magnetic field  $\mathbf{B} = (0, 0, B)$ , the single-particle Hamiltonian is exactly solvable with the single-particle wave function

$$\begin{aligned} \langle \mathbf{x}, \sigma | N, k_x, m_s \rangle &= \Psi_{Nk_x m_s}(\mathbf{x}, \sigma) \\ &= \frac{1}{\sqrt{L_x}} e^{ik_x x} \Phi_N(y - Y_{k_x}) \varphi(z) \chi_{m_s}(\sigma), \end{aligned}$$

where  $\mathbf{x}$  is the spatial and  $\sigma$  the spin coordinate,  $\{|N, k_x, m_s\rangle\}$  is the complete set of single-particle states in the relevant Hilbert space,  $L_x$  is the length of the wire in the  $x$  direction, assuming Born-von-Kármán periodic boundary conditions,  $\Phi_N(y - Y_{k_x})$  is the displaced-center harmonic-oscillator wave function with  $N=0, 1, 2, \dots$  the subband index,  $|\varphi(z)|^2 = \delta(z)$ , and  $\chi_{m_s}(\sigma) = \delta_{\sigma m_s}$  is the  $\sigma$ th component of the eigenspinor  $[\chi]_{m_s} = \begin{pmatrix} \chi_{m_s}^{(+1/2)} \\ \chi_{m_s}^{(-1/2)} \end{pmatrix}$ , where  $m_s = \pm 1/2$  ( $\equiv \uparrow \downarrow$ ) is the spin quantum number. The center coordinate is  $Y_{k_x} = \gamma \tilde{l}_0^2 k_x$ , where  $\gamma = \omega_c / \tilde{\omega}_c$ ,  $\omega_c = eB/m_e$  is the cyclotron frequency,  $\tilde{\omega}_c = (\omega_c^2 + \Omega^2)^{1/2}$  is the hybrid frequency,  $\tilde{l}_0 = [\hbar / (m_e \tilde{\omega}_c)]^{1/2}$  is the typical width of the wave function in the  $y$  direction, and  $k_x$  is the  $x$  component of the electron wave vector. The associated energy eigenvalues are

$\mathcal{E}_{N m_s}(k_x) = \mathcal{E}_N + \hbar^2 k_x^2 / (2\tilde{m}_e) + g^* \mu_B B m_s$ , where  $\mathcal{E}_N = \hbar \tilde{\omega}_c (N + 1/2)$ ,  $\tilde{m}_e = m_e (\tilde{\omega}_c / \Omega)^2 = m_e / (1 - \gamma^2)$  is the magnetic-field-dependent effective mass,  $\mu_B = e \hbar / (2m_0)$  denotes Bohr's magneton with  $m_0$  the free (bare) electron mass, and  $g^*$  is the effective spin-splitting factor.

The energy levels  $\mathcal{E}_{N m_s}(k_x)$  of an electron are shifted by the interaction with the long-wavelength optical phonons. For simplicity we will assume that the electrons inside the QWW only interact with 3D bulk LO phonons. The Hamiltonian of the magnetopolaron,  $\hat{H}_p = \hat{H}_e + \hat{H}_{ph} + \hat{H}_{ep}$ , is

$$\begin{aligned} \hat{H}_p = & \sum_{\alpha} \int d^3x \hat{\Psi}_{\alpha}^{\dagger}(\mathbf{x}) \left\{ \frac{\mathbf{p}_e^2}{2m_e} - \omega_{cy} p_{e_x} + \frac{m_e}{2} \tilde{\omega}_c^2 y^2 + V(z) \right. \\ & + \frac{g^*}{2} \mu_B B \sigma_z + \sum_{\mathbf{q}} \hbar \omega_L [\hat{a}_L^{\dagger}(\mathbf{q}) \hat{a}_L(\mathbf{q}) + \frac{1}{2}] \\ & \left. + \frac{M_0}{V_G^{1/2}} \sum_{\mathbf{q}} e^{i\mathbf{q} \cdot \mathbf{x}} \frac{1}{|\mathbf{q}|} [\hat{a}_L(\mathbf{q}) + \hat{a}_L^{\dagger}(-\mathbf{q})] \right\} \hat{\Psi}_{\alpha}(\mathbf{x}), \quad (1) \end{aligned}$$

where  $\hbar \omega_L$  is the LO phonon energy,  $\hat{a}_L(\mathbf{q})$  and  $\hat{a}_L^{\dagger}(\mathbf{q})$  are the phonon destruction and creation operators, respectively,  $\mathbf{q} = (q_x, q_y, q_z)$  is the 3D wave vector of the LO phonons,  $V_G = L_x L_y L_z$  is the (unit) volume of the sample, and  $M_0 = [4\pi\alpha_p r_p (\hbar \omega_L)^2]^{1/2}$  with the dimensionless 3D polaron coupling constant

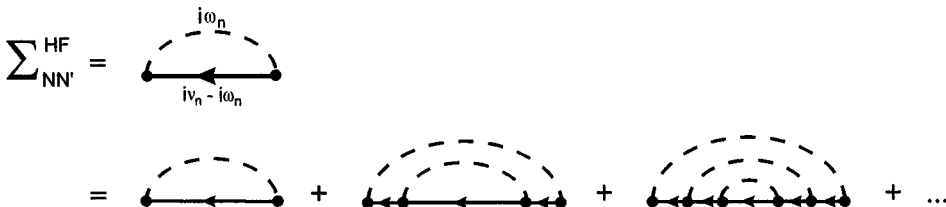
$$\alpha_p = \frac{1}{2} \frac{e^2}{4\pi\epsilon_0 r_p} \left( \frac{1}{\epsilon_{\infty}} - \frac{1}{\epsilon_s} \right) \frac{1}{\hbar \omega_L}$$

and the polaron radius  $r_p = [\hbar / (2m_e \omega_L)]^{1/2}$ . Herein,  $\epsilon_{\infty}$  and  $\epsilon_s$  are the high-frequency (optical) and the static dielectric constant, respectively, and  $\epsilon_0$  is the permittivity in vacuum. Further,  $\hat{\psi}_{\alpha}^{\dagger}(\mathbf{x})$  and  $\hat{\psi}_{\beta}(\mathbf{x})$  are the electron field operators, which can be represented by the closed set of single-particle states of the QWW and  $\alpha, \beta$  are spin coordinates, used quite generally as spin indices because of the chosen  $\{\sigma_z\}$  representation. Dyson's equation for the retarded single-particle (temperature) Green's function  $G_{\alpha\beta}^R(\mathbf{x}, \mathbf{x}' | E)$  becomes in the subband space a matrix equation<sup>18</sup>

$$\begin{aligned} G_{\alpha\beta}^R(k_x, E) = & G_{\alpha\beta}^{(0)R}(k_x, E) + \sum_{N_1, N_1'} \sum_{\sigma, \sigma'} G_{NN_1}^{(0)R}(k_x, E) \\ & \times \sum_{\sigma, \sigma'}^R G_{N_1 N_1'}^R(k_x, E) G_{N_1' \beta}^R(k_x, E). \quad (2) \end{aligned}$$

Herein,

$$G_{\alpha\beta}^{(0)R}(k_x, E) = \frac{\delta_{\alpha\beta} \delta_{NN'}}{E - \mathcal{E}_{N\alpha}(k_x) + \mu + i\delta} \quad (3)$$



is the unperturbed (noninteracting) matrix Green's function, where  $\mu$  is the chemical potential,  $\delta \rightarrow 0^+$ , and  $\sum_{N_1, N_1'}^R(k_x, E)$

is the irreducible (or proper) retarded self-energy. Because in the case considered here the spin is a good quantum number, the matrix Green's function is diagonal in the spin indices:  $G_{\alpha\beta}^R(k_x, E) = \delta_{\alpha\beta} G_{NN';\alpha}^R(k_x, E)$ . Then, Eq. (2) can be transformed in the form

$$\begin{aligned} \sum_{N_1} (E \delta_{NN_1} - [\mathcal{E}_{N\alpha}(k_x) - \mu] \delta_{NN_1} + \sum_{N_1'}^R G_{NN_1';\alpha}(k_x, E)) \\ \times G_{N_1 N_1';\alpha}^R(k_x, E) = \delta_{NN'}. \quad (4) \end{aligned}$$

With  $M_{NN';\alpha}(k_x, E) = E \delta_{NN'} - [\mathcal{E}_{N\alpha}(k_x) - \mu] \delta_{NN'} + \sum_{N_1'}^R G_{NN_1';\alpha}(k_x, E)$  the dressed Green's function  $\mathbf{G}^R(k_x, E) \equiv (G_{NN';\alpha}^R(k_x, E))$  is given by the inverse of  $\mathbf{M}(k_x, E)$ :  $\mathbf{G}^R(k_x, E) = \mathbf{M}^{-1}(k_x, E)$ . The quasiparticles, i.e., the Q1D magnetopolarons, are given by the poles of the Green's function  $\mathbf{G}^R(k_x, E)$ . For obvious reasons the matrix Green's function  $G_{NN';\alpha}^R(k_x, E)$  of an electron in a QWW with  $M$  subbands taken into account (an  $M$ -subband model) has  $2M$  isolated single poles at the complex energies  $E = E_{\eta}(k_x) - \mu - i\Gamma_{\eta}(k_x)$ ;  $\eta = 1, 2, 3, \dots, 2M$  connected with subband ( $N = 0, 1, 2, \dots, M-1$ ) and spin index ( $\alpha = \pm \frac{1}{2}$ ). From the theory of complex functions it follows that the matrix Green's function can be represented near the quasiparticle poles in the following form:<sup>19</sup>

$$G_{NN';\alpha}^R(k_x, E) \approx \sum_{\eta=1}^{2M} \frac{z_{\eta}^{NN';\alpha}(k_x)}{E - E_{\eta} + \mu + i\Gamma_{\eta}(k_x)}, \quad (5)$$

where the so-called renormalization factors  $z_{\eta}^{NN';\alpha}(k_x)$  are the residues of  $G_{NN';\alpha}^R(k_x, E)$  at the poles  $E = E_{\eta}(k_x) - \mu - i\Gamma_{\eta}(k_x)$ . If and only if  $\Gamma_{\eta} \ll |E_{\eta} - \mu|$  is valid, i.e., the poles occur very close to the real energy axis, are the above states true quasiparticle states. Their energies and damping functions are then determined from the equation

$$\det [M_{NN';\alpha}(k_x, E_{\eta} - \mu - i\Gamma_{\eta}) |_{\Sigma_{NN';\alpha}(k_x, E_{\eta} - \mu)}] = 0, \quad (6)$$

where in the matrix elements of the self-energy, which occur in  $M_{NN';\alpha}(k_x, E)$  according to the quasiparticle picture,  $\Gamma_{\eta} \rightarrow 0$  is assumed. The renormalization factor reads

$$z_{\eta}^{NN';\alpha}(k_x) = \text{Res}_{E=E_{\eta}(k_x) - \mu} \{[\mathbf{M}^{-1}(k_x, E)]_{NN';\alpha}\}, \quad (7)$$

where  $(\mathbf{M}^{-1})_{NN';\alpha}$  denotes the  $(NN';\alpha)$ th element of  $\mathbf{M}^{-1}$ , Res means the residue at the pole, and in the self-energy  $\Gamma_{\eta} \rightarrow 0$  is assumed. If the quasiparticle damping is vanishingly small, the Lorentz profiles of the spectral function  $A_{NN';\alpha}(k_x, E)$  at the quasiparticle energies

FIG. 1. Feynman diagrams which are included in the irreducible Hartree-Fock matrix self-energy  $\Sigma_{NN';\alpha}^{\text{HF}}(k_x, i\nu_n)$  of the interacting electron-phonon system in QWW's.

$$A_{NN';\alpha}(k_x, E) \approx \frac{1}{\pi} \sum_{\eta=1}^{2M} \frac{z_{\eta}^{NN';\alpha}(k_x) \Gamma_{\eta}(k_x)}{[E - E_{\eta}(k_x) + \mu]^2 + \Gamma_{\eta}^2(k_x)}, \quad (8)$$

become sharp delta peaks:

$$A_{NN';\alpha}(k_x, E) \approx \sum_{\eta=1}^{2M} z_{\eta}^{NN';\alpha}(k_x) \delta(E - E_{\eta}(k_x) + \mu). \quad (9)$$

In the quasiparticle approximation (QPA) one uses this matrix spectral function in the whole spectrum and, thus, in this approach the sum rule

$$\sum_{\eta=1}^{2M} z_{\eta}^{NN';\alpha}(k_x) = \delta_{NN'} \quad (10)$$

becomes valid. From the energy-momentum relation  $E_{\eta}(k_x)$  one can calculate the magnetopolaron effective mass  $\tilde{m}_{\eta}^*$  of the quasiparticle state  $|\eta, k_x\rangle$ :

$$\frac{1}{\tilde{m}_{\eta}^*} = \lim_{k_x \rightarrow 0} \frac{1}{k_x \hbar^2} \frac{d}{dk_x} E_{\eta}(k_x). \quad (11)$$

Let us now calculate the matrix self-energy in the framework of the Hartree-Fock approximation (HFA) using the Matsubara technique for the temperature Green's function. The Feynman diagram of the irreducible HF self-energy is shown in Fig. 1 and given by

$$\Sigma_{NN';\alpha}^{\text{HF}}(k_x, i\nu_n) = \frac{1}{L_x} \sum_{q_x} \sum_{N_1 N_1'} \left( -\frac{1}{\beta} \right) \sum_{i\omega_n} V_{N_1 N_1'}^{\text{ph}}(q_x, i\omega_n) \mathcal{G}_{N_1 N_1';\alpha}(k_x - q_x, i\nu_n - i\omega_n), \quad (12)$$

where the (Matsubara) frequencies are  $\omega_n = 2\pi n / (\beta\hbar)$  and  $\nu_n = \pi(2n+1) / (\beta\hbar)$  with  $n = 0, \pm 1, \pm 2, \dots$  and  $\beta = 1/(k_B T)$ , where  $k_B$  is Boltzmann's constant. The electron-phonon interaction potential in subband space is<sup>18,20</sup>

$$V_{N_1 N_2 N_3 N_4}^{\text{ph}}(q_x, i\omega_n) = f_{N_1 N_2 N_3 N_4}^{\text{LO}}(q_x) \frac{2\omega_L / \hbar}{(i\omega_n - \omega_L)(i\omega_n + \omega_L)}, \quad (13)$$

where the form factor  $f_{N_1 N_2 N_3 N_4}^{\text{LO}}(q_x)$  is given by

$$f_{N_1 N_2 N_3 N_4}^{\text{LO}}(q_x) = 2\alpha_p r_p (\hbar\omega_L)^2 \int_{-\infty}^{\infty} dy \int_{-\infty}^{\infty} dy' \Phi_{N_1}^*(y - Y_{k_x+q_x}) \Phi_{N_2}(y - Y_{k_x}) K_0[|q_x(y-y')|] \\ \times \Phi_{N_3}^*(y' - Y_{k'_x-q_x}) \Phi_{N_4}(y' - Y_{k'_x}), \quad (14)$$

with  $K_0[|q_x(y-y')|]$  the modified Bessel function of zeroth order (for calculation and result see Ref. 21). Note that the lower indices of the form factor denote the center coordinates of the single-particle electron wave function. Explicit calculation of  $f_{N_1 N_2 N_3 N_4}^{\text{LO}}(q_x)$  shows that this form factor is independent of the wave-vector components  $k_x$  and  $k'_x$ . The electron-phonon interaction may be interpreted as a phonon-mediated electron-electron interaction potential. Such an interaction potential signifies the scattering of an electron from subband  $N_2$  to  $N_1$  by another electron, which becomes scattered from subband  $N_4$  to  $N_3$  by exchanging a LO phonon. The frequency sum in Eq. (12) can be easily performed with the result

$$\Sigma_{NN';\alpha}^{\text{HF}}(k_x, E) = \frac{1}{L_x} \sum_{q_x} \sum_{N_1 N_1'} f_{N_1 N_2 N_3 N_4}^{\text{LO}}(q_x) \{ [n_B(\omega_L) + 1] G_{N_1 N_1';\alpha}^R(k_x - q_x, E - \hbar\omega_L) \\ + n_B(\omega_L) G_{N_1 N_1';\alpha}^R(k_x - q_x, E + \hbar\omega_L) \}, \quad (15)$$

where  $G^R(k_x, E)$  is the dressed retarded HF Green's function and  $n_B(\omega_L) = [e^{\beta\hbar\omega_L} - 1]^{-1}$  is the Bose occupancy factor for the LO phonons. This Green's function has to be calculated self-consistently from Eqs. (4) and (15). This is the general HF result for the EPI in QWW's in the presence of a magnetic field. The HF self-energy  $\Sigma_{NN';\alpha}^{\text{HF}}(k_x, E)$ , with  $G_{NN';\alpha}^R(k_x, E)$  in terms of  $\Sigma_{NN';\alpha}^{\text{HF}}(k_x, E)$  via Dyson's equation, Eq. (4), is then given by a very complicated matrix equation, including an integral equation for  $q_x$  and a difference equation in frequency. Because we are mostly interested in the quasiparticle properties here,

it is more profitable to perform the frequency sum over  $i\omega_n$  in Eq. (12) by using the QPA for the dressed Green's function (I call this internal QPA). Then, we obtain for the retarded self-energy

$$\Sigma_{NN';\alpha}^{\text{HF}}(k_x, E) = \frac{1}{L_x} \sum_{q_x} \sum_{N_1 N_1'} \sum_{k_x k_x - q_x}^{\text{LO}} \sum_{N_1' N_1'} f_{k_x k_x - q_x}^{N_1 N_1'}(q_x) \sum_{\eta=0}^{2M} z_{\eta}^{N_1 N_1';\alpha}(k_x - q_x) \left\{ \frac{n_B(\omega_L) + 1}{E - E_{\eta}(k_x - q_x) - \hbar\omega_L + i\delta} + \frac{n_B(\omega_L)}{E - E_{\eta}(k_x - q_x) + \hbar\omega_L + i\delta} \right\}, \quad (16)$$

assuming now for simplicity a single electron in the QWW by changing  $i\hbar\nu_n \rightarrow E - \mu + i\delta$  in the final result. In this equation,  $E_{\eta}(k_x - q_x)$  is a solution of Eq. (6) and  $z_{\eta}^{N_1 N_1';\alpha}(k_x - q_x)$  is determined by Eq. (7) and fulfills the sum rule (10). Equation (16) generalizes our earlier result<sup>22</sup> to the case that all possible intersubband processes are included. The first term in the curly brackets comes from the emission of a LO phonon by the electron and the second term, which vanishes at zero temperature, is connected with the absorption of a LO phonon. A nonvanishing imaginary part results from the emission and absorption of real LO phonons. At  $T=0$  and for  $E < \hbar\omega_L$  there are no real LO phonons available and thus, the true magnetopolaron states are zero-phonon magnetopolaron states.

The general  $n$ -phonon magnetopolaron state is described by the set  $|\eta, k_x^{\text{pol}}; \{n_{\mathbf{q}}\}\rangle = |\eta, k_x^{\text{pol}}\rangle \otimes |\{n_{\mathbf{q}}\}\rangle$ , where  $|\{n_{\mathbf{q}}\}\rangle = \prod_{\mathbf{q}} (1/\sqrt{n_{\mathbf{q}}!}) [(a_{L}^{\dagger}(\mathbf{q}))^{n_{\mathbf{q}}}] |0\rangle$  is the state vector of the LO phonons, with  $n_{\mathbf{q}}$  LO phonons in each mode, each with momentum  $\hbar\mathbf{q}$  and energy  $\hbar\omega_L$  and  $k_x^{\text{pol}} = k_x + \sum_{\mathbf{q}} q_x n_{\mathbf{q}}$  is the magnetopolaron wave vector component along the wire axis. For the zero-phonon magnetopolaron state  $|\eta, k_x^{\text{pol}} = k_x; 0_{\mathbf{q}}\rangle$  is valid. Thus, in the case investigated here the renormalization is due to virtual LO-phonon emission and reabsorption processes only. Only a finite number of renormalized subbands will lie in the region  $E < \hbar\omega_L$ , which have a unique energy-momentum relation: there is only one state for each subband at a given energy. This picture is drastically changed for the one-phonon magnetopolaron states  $|\eta, k_x^{\text{pol}} = k_x + q_x; 1_{\mathbf{q}}\rangle$ . Due to the different possible  $q_x = 2\pi n_x/L_x$ ;  $n_x = 0, \pm 1, \pm 2, \dots$  there is a quasicontinuum of states. The lower boundary of this phonon continuum has the threshold energy  $E_{\text{th}}^{(\eta)} = \min\{E_{\eta}(k_x + q_x) + \hbar\omega_L\} = E_{\eta}(0) + \hbar\omega_L$ , which is independent from  $k_x$  but depends on the magnetic field. Each zero-phonon magnetopolaron state  $|\eta, k_x^{\text{pol}} = k_x; 0_{\mathbf{q}}\rangle$  is accompanied by its one-, two-, three-phonon, etc. continuum. Thus, the phonon continuum of all states exists above the threshold of the one-phonon continuum of the energetically lowest-lying state. Because the electron-phonon interaction is independent from the electron spin, the self-energy given by Eq. (16) is indeed independent from the spin index too. The Zeeman energy only scales the quasiparticle energy, i.e., it may be dropped by redefining  $E$ . Thus, spin-up and spin-down electrons are independent and each group may be considered separately. Henceforth, two different threshold energies  $E_{\text{th}}^{(\uparrow)}$  and  $E_{\text{th}}^{(\downarrow)}$  of the two-phonon continua arise for all spin-up and all spin-down electrons, respectively.

Considering for the moment the energy-momentum relation  $\mathcal{E}_{N\alpha; n_{\mathbf{q}}}(k_x^{\text{pol}}; B) = \hbar\tilde{\omega}_c(N + 1/2) + g^* \mu_B B \alpha + (\hbar^2/2\tilde{m}_e)(k_x^{\text{pol}} - \sum_{\mathbf{q}} q_x n_{\mathbf{q}})^2 + \sum_{\mathbf{q}} \hbar\omega_L n_{\mathbf{q}}$  for the  $n$ -phonon unperturbed magnetopolaron state  $|N, k_x^{\text{pol}}, \alpha; \{n_{\mathbf{q}}\}\rangle$ , the renormalized phonon continuum is above the threshold energy  $\mathcal{E}_{\text{th}}^{(\alpha)} = \mathcal{E}_{\text{th}}^{(\alpha)}(B) = \hbar\tilde{\omega}_c/2 + \hbar\omega_L + g^* \mu_B B \alpha$ . Obviously, without the interaction the zero-phonon magnetopolaron dispersion curves with bottoms that occur for  $k_x = 0$  below  $\mathcal{E}_{\text{th}}^{(\alpha)}$ , i.e., if  $N\tilde{\omega}_c < \omega_L$ , would cross this line with increasing wave vector at  $k_x = k_L^{(N)} = [(2\tilde{m}_e/\hbar)(\omega_L - N\tilde{\omega}_c)]^{1/2}$ . Further, the zero-phonon magnetopolaron unperturbed states with  $N > 0$  and bottoms below  $\mathcal{E}_{\text{th}}^{(\alpha)}$ , i.e., if  $N\Omega < \omega_L$  is valid for  $B = 0$ , cross with increasing magnetic field the lower boundary of the one-phonon continuum at

$$\omega_c = \omega_c^{(N)} = \left\{ \left[ \frac{1}{N} \left( \omega_L - \frac{\hbar k_x^2}{2\tilde{m}_e} \right) \right]^2 - \Omega^2 \right\}^{1/2}.$$

In this case also the unshifted level  $\mathcal{E}_{0\alpha; 0}(k_x; B)$  crosses  $\mathcal{E}_{\text{th}}^{(\alpha)}$  at  $\omega_c = \omega_c^{(0)} = \Omega[(k_x r_p)^2 - 1]^{1/2}$  but only if  $k_x r_p \geq 1$ . For levels  $\mathcal{E}_{N\alpha; 0_{\mathbf{q}}}(0; B)$  with  $\omega_L \leq N\Omega$  there is no crossing with the line  $\mathcal{E}_{\text{th}}^{(\alpha)}$  with increasing magnetic field and for  $\omega_L \leq N\tilde{\omega}_c$  the same is true for increasing wave vector. Thus, there are two different ways to cross the lower boundary  $\mathcal{E}_{\text{th}}^{(\alpha)}$  of the one-phonon continuum: one with increasing magnetic field and the other one with increasing kinetic energy. As known, in 3D and strict 2D systems the magnetopolaron behavior is quite different on these two ways. Hence, with increasing magnetic field and wave vector the zero-phonon levels with bottoms below the threshold energy,  $\mathcal{E}_{N\alpha; 0_{\mathbf{q}}}(0; 0) < \mathcal{E}_{\text{th}}^{(\alpha)}$ , become degenerate with the continuous states inside the one-phonon continuum. But the perturbation that couples each state with the phonon continuum will lead to a splitting of each zero-phonon magnetopolaron energy-momentum relation with one branch below and one branch inside the phonon continuum. Thus, all zero-phonon magnetopolaron states with energy bottoms below the threshold of the renormalized phonon continuum at  $E_{\text{th}}^{(\alpha)}$  must bend over at the associated threshold energy for spin-up and spin-down electrons if their energies approach with increasing momentum and magnetic field the lower boundary  $E_{\text{th}}^{(\alpha)}$  of the one-phonon continuum because of the anticrossing repulsion of the levels. For larger momenta and/or magnetic fields these states are then pinned

at this line. This effect is called resonant magnetopolaron level coupling (RMPLC) and the associated quasiparticle state is called resonant magnetopolaron.

In general, the numerical calculation of the self-energy in the form of Eq. (16) is possible but very cumbersome. Thus, we will look for further suitable approximations. At first it is profitable to perform a diagonal approximation for the dressed Green's function in Eq. (12), i.e., to set  $\mathcal{G}_{NN';\alpha}(k_x, i\nu_n) \Rightarrow \delta_{NN'} \mathcal{G}_{NN;\alpha}(k_x, i\nu_n)$ . I call this an internal diagonal approximation, because in this case the resulting self-energy as well as the Green's function given by Dyson's equation remain nondiagonal matrices. The internal diagonal

approximation is well justified in most cases, because the nondiagonal matrix elements are usually only 1–10% in magnitude of the diagonal ones. In the case of the internal diagonal approximation, from Eq. (4) it follows that  $G_{NN;\alpha}^R(k_x, E) = [E - \mathcal{E}_{N\alpha}(k_x) - \Sigma_{NN;\alpha}^R(k_x, E)]^{-1}$  for the matrix Green's function and, thus, quasiparticle energies and damping function are determined by  $E_{N\alpha}(k_x) = \mathcal{E}_{N\alpha}(k_x) + \text{Re}\Sigma_{NN;\alpha}^R(k_x, E_{N\alpha}(k_x))$  and  $\Gamma_{N\alpha}(k_x) = -\text{Im}\Sigma_{NN;\alpha}^R(k_x, E_{N\alpha}(k_x))$ , respectively. In the QPA spectral function in the diagonal approximation is  $A_{NN;\alpha}(k_x, E) = \delta(E - E_{N\alpha}(k_x))$ . Applying this internal diagonal approximation to Eq. (16) and assuming  $T=0$ , we obtain

$$\Sigma_{NN';\alpha}^{\text{HF}}(k_x, E) = \frac{1}{L_x} \sum_{q_x} \sum_{N_1} \frac{f_{N_1}^{\text{LO}}(q_x)}{E - \mathcal{E}_{N_1\alpha}(k_x - q_x) - \text{Re}\Sigma_{N_1N_1;\alpha}^{\text{HF}}[k_x - q_x, E_{N_1\alpha}(k_x - q_x)] - \hbar\omega_L + i\delta}. \quad (17)$$

This self-energy combined with Eq. (6) determines the quasiparticle properties of the Q1D magnetopolaron in the framework of the HFA. Setting  $\text{Re}\Sigma_{N_1N_1;\alpha}^{\text{HF}} = 0$  in the denominator gives the Tamm-Dancoff approximation (TDA) for the self-energy. This result follows directly from the first-order self-energy Feynman graph depicted in Fig. 1:  $\Sigma_{NN';\alpha}^{\text{TDA}}(k_x, E) \equiv \Sigma_{NN';\alpha}^{(1)R}(k_x, E)$ . Comparing the HFA with the TDA it becomes obvious that the HF self-energy contains the same scattering processes as in the Tamm-Dancoff case but between the renormalized subband energies. Thus, from the point of view of the EPI, the HF approach given by Eq. (17) is an improved Tamm-Dancoff approximation (ITDA). It is known (see, e.g., Ref. 16) that the TDA gives the wrong pinning behavior of the zero-phonon magnetopolaron energy-momentum relations at the one-phonon energy  $\hbar\omega_L$  above the unrenormalized ground state  $\mathcal{E}_0(0;B)$ .

In principle, the HF matrix self-energy of Eq. (17) may be calculated numerically. However, this is a very cumbersome procedure because for the calculation of each matrix element all the other matrix elements must be known from the foregoing step of the self-consistent procedure. Thus, it is profitable to perform a further simplifying approximation. However, this approximation of the HF self-energy of Eq. (17) shall be an improved TDA and, therefore, it has to fulfill two requirements. Firstly, for  $k_x \rightarrow 0$  the matrix self-energy of the ground state should approach the corresponding matrix self-energy calculated on-mass shell [OMS:  $E = \mathcal{E}_{0\alpha}(k_x)$  in  $\text{Re}\Sigma_{00;\alpha}^{\text{TDA}}(k_x, E) \Rightarrow \text{Re}\Sigma_{00;\alpha}^{\text{OMS}}(k_x)$ ]. Secondly, for large  $k_x$  the matrix self-energy should give the correct pinning behavior of the zero-phonon magnetopolaron energy-momentum relations at the one-phonon energy  $\hbar\omega_L$  above the renormalized ground state  $E_0(0;B)$ . From Eq. (17) it becomes obvious that the real part of the HF self-energy at the quasiparticle energies shows the energetically lowest resonance at  $E_\eta(k_x) = \mathcal{E}_{0\alpha}(0) + \text{Re}\Sigma_{00;\alpha}^{\text{HF}}[0, E_{0\alpha}(0)] + \hbar\omega_L$  because the phonon wave vector component  $q_x$  can take all possible values. Therefore, it should be a reasonable approach to set

$\text{Re}\Sigma_{N_1N_1;\alpha}^{\text{HF}}[k_x - q_x, E_{N_1\alpha}(k_x - q_x)] \Rightarrow \text{Re}\Sigma_{00;\alpha}^{\text{HF}}[0, E_{0\alpha}(0)]$  in the denominator of Eq. (17). I call Eq. (17) with  $\text{Re}\Sigma_{N_1N_1;\alpha}^{\text{HF}}[k_x - q_x, E_{N_1\alpha}(k_x - q_x)] \Rightarrow \text{Re}\Sigma_{00;\alpha}^{\text{HF}}[0, E_{0\alpha}(0)]$  in the denominator together with Eq. (6) the modified Hartree-Fock approximation (MHFA) for the interacting electron-phonon system in the subband space. Let us discuss the physical meaning of this approach in detail. In the MHFA we use in the calculation of the matrix self-energy, when starting from Eq. (15), instead of the exact dressed HF Green's function  $G_{NN';\alpha}^R(k_x, E)$  an approximated one:  $G_{NN';\alpha}^R(k_x, E) = \delta_{NN'} / \{E - \mathcal{E}_{N\alpha}(k_x) - \Sigma_{00;\alpha}^{\text{HF}}[0, E_0(0)]\}$ . It becomes obvious that the MHFA exactly fulfills the first requirement (see also discussion below). The MHF self-energy simplifies the HF self-energy, Eq. (17), twofold: (i) At first it is assumed as the starting point of the self-consistent calculation of the matrix self-energy that the renormalization is the same for all levels. (ii) Secondly, for the reference levels  $E_{N_1\alpha}(k_x - q_x) + \hbar\omega_L = \mathcal{E}_{N_1\alpha}(k_x - q_x) + \text{Re}\Sigma_{N_1N_1;\alpha}^{\text{HF}}[k_x - q_x, E_{N_1\alpha}(k_x - q_x)] + \hbar\omega_L \approx \mathcal{E}_{N_1\alpha}(k_x - q_x) + \text{Re}\Sigma_{00;\alpha}^{\text{HF}}[0, E_{0\alpha}(0)] + \hbar\omega_L$  the pinning at  $E_{N_1\alpha}(0) + 2\hbar\omega_L$  is neglected. As described above the denominator of the fraction  $1/\{E_\eta(k_x) - [E_{N_1\alpha}(k_x - q_x) + \hbar\omega_L]\}$  is responsible for electron scattering between  $E_\eta$  and  $E_{N_1\alpha} + \hbar\omega_L$ . Assuming for the moment  $E_\eta$  and  $k_x$  to be fixed, the most important contributions to the self-energy  $\Sigma_{NN';\alpha}^{\text{HF}}$  result from the electron scattering between  $E_\eta$  and the energetically lowest reference levels, i.e., the reference levels  $E_{0\alpha}(k_x - q_x) + \hbar\omega_L$ . As shown above,  $E_{0\alpha}(k_x - q_x) + \hbar\omega_L$  bends over at  $E_{0\alpha}(0) + 2\hbar\omega_L$ . Because the self-energy is nearly independent from the wave vector,  $\text{Re}\Sigma_{00;\alpha}^{\text{HF}}[k_x - q_x, E_{0\alpha}(k_x - q_x)] \approx \text{Re}\Sigma_{00;\alpha}^{\text{HF}}[0, E_{0\alpha}(0)]$ , as long as the energy is below the bend-over region [see, e.g., Fig. 5(a) below], the sum over all quasicontinuous values of  $q_x$  gives a sum of fractions  $1/\{E_\eta(k_x) - [E_{0\alpha}(k_x - q_x) + \hbar\omega_L]\}$ , in which the most important large terms, arising from energies below of  $E_{0\alpha}(0) + 2\hbar\omega_L$ , are correct in the

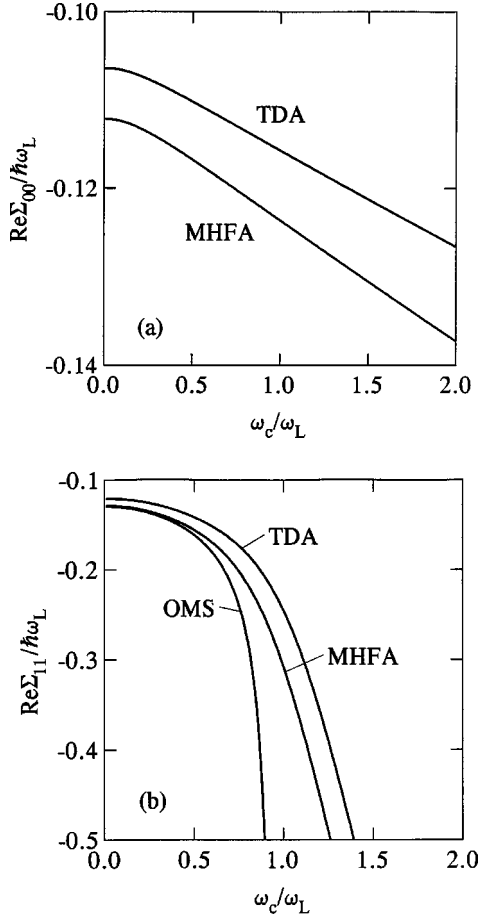


FIG. 2. The matrix self-energies  $\text{Re}\Sigma_{00}$  (a) and  $\text{Re}\Sigma_{11}$  (b) of the Q1D subbands  $\mathcal{E}_0$  and  $\mathcal{E}_1$ , respectively, for  $k_x=0$  as a function of the magnetic field calculated in MHFA, TDA, and TDA on-mass shell (OMS).

MHFA. Only the unimportant smallest terms (i.e., the smallest fractions in the sum over  $q_x$ ), arising for energies in the bend-over region of the reference levels,  $E_{0\alpha}(k_x - q_x) + \hbar\omega_L \approx E_{0\alpha}(0) + 2\hbar\omega_L$ , are in the MHFA smaller than in the HFA. Thus, compared with the HFA, the MHFA slightly underestimates the EPI self-energy, but this is a negligibly small effect. This is true because of the quasicontinuum of states according to the different  $q_x$ , we have for a given  $k_x$  a quasi-infinite number of correct states, which have the largest contribution to the self-energy. For this reason, the energetically higher states,  $N_1 > 0$ , give only a minor contribution to the self-energy, so that part (i) of the approximations has practically no consequence for the numerical value of the matrix self-energy. Thus, we can conclude that the MHFA drastically simplifies the calculation of the matrix self-energy but still gives highly accurate results especially for the lower subbands and, most important, it results in the correct pinning behavior of the zero-phonon magnetopolaron dispersion relations. Compared with the exact HFA, the MHFA is computationally much simpler and highly efficient.

The numerical calculation we have applied to a GaAs-Ga<sub>1-x</sub>Al<sub>x</sub>As QWW with the material parameters  $\alpha_p = 0.07$ ,  $r_p = 3.987$  nm,  $\hbar\omega_L = 36.17$  meV,  $m_e = 0.06624m_0$  for GaAs and for the confinement energy  $\hbar\Omega = 12$  meV is used. For the chosen parameters the nondiagonal elements of the

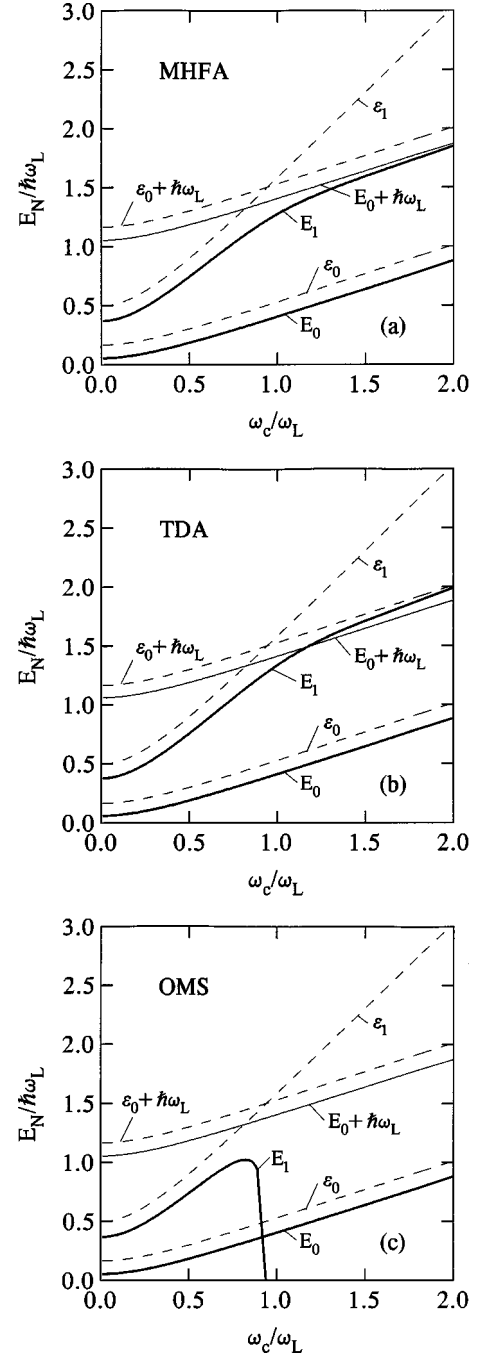


FIG. 3. Dependence of the renormalized levels  $E_0$ ,  $E_1$  (heavy solid lines) and  $E_0 + \hbar\omega_L$  (thin solid line) and of the unrenormalized levels  $\mathcal{E}_0$ ,  $\mathcal{E}_1$ , and  $\mathcal{E}_0 + \hbar\omega_L$  (dashed lines) on the magnetic field: (a) calculated in MHFA, (b) in TDA, and (c) in OMS.

matrix self-energy are small compared to the diagonal elements and, thus, the diagonal approximation is a suitable approach to calculate the magnetopolaron dispersion relation  $E_{N\alpha}(k_x)$ . Note that with decreasing confining energy the contribution of the nondiagonal elements to the quasiparticle properties increases. With these approximations the real part of the MHF self-energy of Eq. (17) can be written at the real quasiparticle energies  $E = E_N(k_x)$  below the phonon continuum, introducing 3D polaron units (energies are measured in units of  $\hbar\omega_L$  and lengths in units of  $r_p$ ), in the form

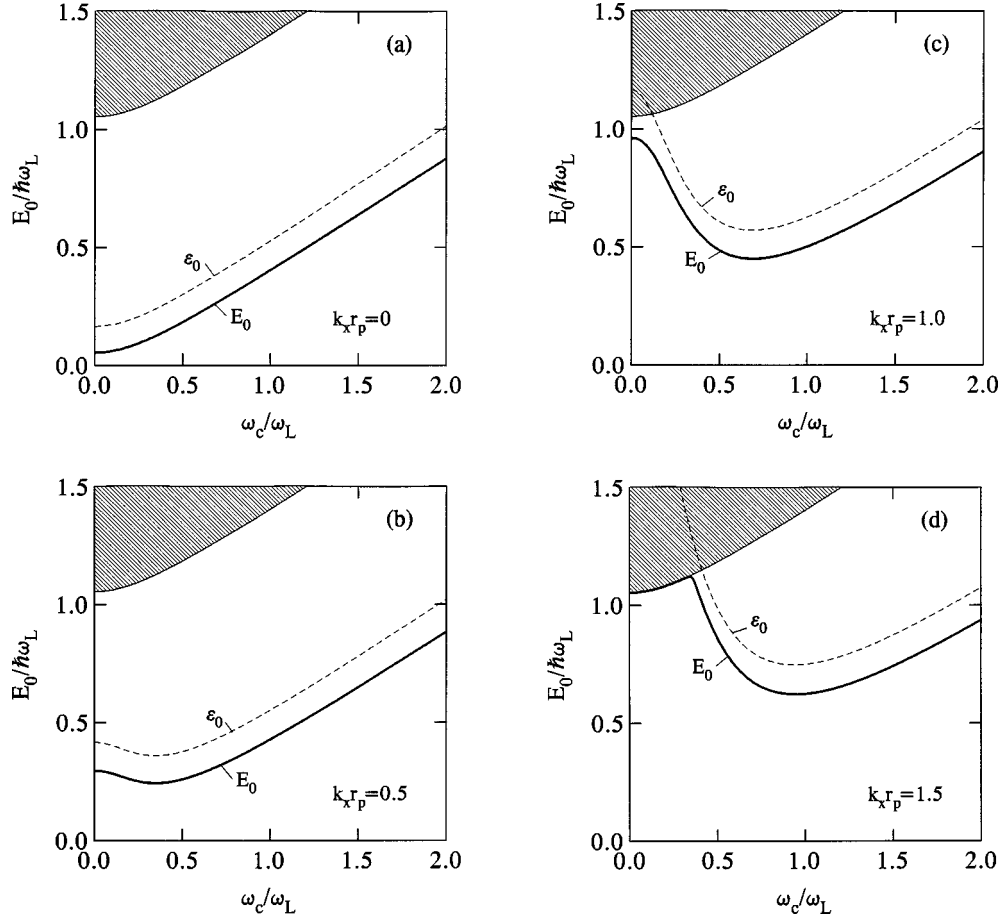


FIG. 4. The lowest QID magnetopolaron level  $E_0(k_x; B)$  (heavy solid line) as a function of the magnetic field for different magnetopolaron momenta: (a)  $k_x r_p = 0$ ; (b)  $k_x r_p = 0.5$ ; (c)  $k_x r_p = 1.0$ , and (d)  $k_x r_p = 1.5$  calculated in MHFA. The corresponding unperturbed dispersion relation  $\epsilon_0(k_x; B)$  is plotted by the dashed line. The renormalized phonon continuum is shown by the hatched area.

$$\text{Re}\Sigma_{NN}^{\text{MHF}}[k_x, E_N(k_x)]$$

$$\begin{aligned}
&= -\frac{\alpha_p}{2\pi} \int_0^\infty dq_{\parallel} \int_{-\pi}^{\pi} d\varphi e^{-a} \int_0^\infty dt \exp\{-[1 - \lambda^2 N \\
&\quad + (1 - \gamma^2) q_{\parallel}^2 \cos^2 \varphi - 2(1 - \gamma^2) k_x q_{\parallel} \cos \varphi \\
&\quad - \Delta_{NN}^{\text{MHF}}(k_x)]t\} \sum_{N'=0}^{\infty} \frac{N_2!}{N_1!} a^{N_1 - N_2} \\
&\quad \times [L_{N_2}^{N_1 - N_2}(a)]^2 e^{-\lambda^2 N_1 t}, \quad (18)
\end{aligned}$$

where  $\Delta_{NN}^{\text{MHF}}(k_x) = \text{Re}\Sigma_{NN}^{\text{MHF}}[k_x, E_N(k_x)] - \text{Re}\Sigma_{00}^{\text{MHF}}[0, E_0(0)]$ . Further, we have introduced  $q_{\parallel} = (q_x^2 + q_y^2)^{1/2}$ ,  $\cos \varphi = q_x / q_{\parallel}$ ,  $\sin \varphi = q_y / q_{\parallel}$ ,  $a = (q_{\parallel}^2 / \lambda^2) [1 - (1 - \gamma^2) \cos^2 \varphi]$ ,  $\lambda^2 = \tilde{\omega}_c / \omega_L$ ,  $N_1 = \max(N, N')$ ,  $N_2 = \min(N, N')$  and  $L_N^{N'}(\xi)$  is the associated Laguerre polynomial. By scaling the energy, the Zeeman energy does not occur in this equation. Note further that the spin splitting of the levels is very small compared to the subband separation of 12 meV under consideration, e.g., for  $B_L \equiv m_e \omega_L / e = 20.7$  T, where  $\omega_c = \omega_L$ , we have  $|g^* \mu_B B| = 0.527$  meV for GaAs, where  $g^* = -0.44$ .

The approach for the self-energy in Eq. (18) is identical to the second-order (modified) improved Wigner-Brillouin perturbation theory (IWBPT).<sup>16,17,23</sup> Further, if one takes in Eq.

(18)  $\text{Re}\Sigma_{00}^{\text{MHF}}[0, E_0(0)] = 0$  in  $\Delta_{NN}^{\text{MHF}}(k_x)$ , the result of the TDA in the diagonal approximation follows, which is equivalent to the Wigner-Brillouin perturbation theory (WBPT). If additionally  $\text{Re}\Sigma_{00}^{\text{MHF}}[k_x, E_N(k_x)]$  is set equal to zero in  $\Delta_{NN}^{\text{MHF}}(k_x)$ , which is equivalent to considering the diagonal elements of the first-order self-energy on-mass shell,  $E = \mathcal{E}_N(k_x)$  in  $\text{Re}\Sigma_{NN}^{\text{TDA}}(k_x, E) \Rightarrow \text{Re}\Sigma_{NN}^{\text{OMS}}(k_x)$ , the result of the Rayleigh-Schrödinger perturbation theory (RSPT) follows. From this discussion it becomes obvious that the exact HF Green's-function result, given by Eqs. (15) and (16), and the MHFA include much more intersubband processes than the orthodox perturbation theories. The basic differences between the results for QID magnetopolarons obtained by using the Green's-function technique and by using the old-fashioned perturbation theories are the following: (i) The Feynman-Dyson perturbation theory gives real and imaginary self-energy contributions for intrasubband and intersubband processes, while the old-fashioned perturbation theories give only real self-energy contributions for intrasubband and some intersubband processes. (ii) The matrix self-energy calculated with the Green's-function technique contains scattering processes of two electrons from subbands  $N_1$  to  $N$  and from  $N'$  to  $N_1$ , whereas RSPT, WBPT, and IWBPT include only the symmetric processes of scattering from  $N_1$  to  $N$  and from  $N$  to  $N_1$ . The asymmetric scattering of the two

electrons by exchanging an optical phonon give rise to the nondiagonal elements of the matrix self-energy. (iii) Neglecting these asymmetric scattering processes, the diagonal elements of the real part of the self-energy  $\text{Re}\Sigma_{NN}[k_x, E_N(k_x)]$  at  $T=0$  calculated in MHFA and in TDA become equivalent to the second-order IWBPT and

WBPT, respectively. (iv) The diagonal elements of the TDA matrix self-energy in the mass-shell approximation become the same as in second-order RSPT.

The sum over  $N'$  and the integral over  $q_{\parallel}$  in Eq. (18) can be easily performed analytically. For the renormalization of the lowest subband we obtain from Eq. (18)

$$\begin{aligned} \text{Re}\Sigma_{00}^{\text{MHF}}[k_x, E_0(k_x)] = & -\alpha_p \frac{\lambda}{\sqrt{\pi}} \int_0^{\pi/2} d\varphi \int_0^{\infty} dt e^{-[1-\Delta_{00}^{\text{MHF}}(k_x)]t} \\ & \times \frac{\exp\{\lambda^2 t^2 k_x^2 (1-\gamma^2)^2 \cos^2 \varphi / [1 - e^{-\lambda^2 t} + (1-\gamma^2) \cos^2 \varphi (e^{-\lambda^2 t} + \lambda^2 t - 1)]\}}{\sqrt{1 - e^{-\lambda^2 t} + (1-\gamma^2) \cos^2 \varphi (e^{-\lambda^2 t} + \lambda^2 t - 1)}}. \end{aligned} \quad (19)$$

If the lateral confining potential vanishes, i.e., for  $\Omega=0$  and, thus,  $\gamma=1$  and  $\lambda^2=\omega_c/\omega_L$  in Eq. (18), one derives, e.g., from Eq. (19), the analytical result

$$\text{Re}\Sigma_{00}^{\text{MHF}}|_{2\text{D}} = -\alpha_p \frac{\sqrt{\pi}}{2\lambda} B\left(\frac{1}{\lambda^2}, \frac{1}{2}\right) \quad (20)$$

for the 2D magnetopolaron self-energy, where  $B(x,y)$  is the beta function and obviously  $\Delta_{00}^{\text{MHF}}=0$ . This result was first obtained by Larsen.<sup>4</sup> It becomes obvious that this expression is independent of  $k_x$ . This is true because electrons quantum confined in the  $x$ - $y$  plane are totally quantized in Landau levels in the presence of a perpendicular quantizing magnetic field.

In the case of a vanishing magnetic field ( $B=0$ ), Eq. (18) is valid with  $\gamma=0$ ,  $\lambda^2=\Omega/\omega_L$ , and  $a=(q_{\parallel}^2/\lambda^2)\sin^2\varphi$ , as discussed in detail in Ref. 16. In this case Eq. (19) reads

$$\text{Re}\Sigma_{00}^{\text{MHF}}[k_x, E_0(k_x)] = -\frac{\alpha_p}{\sqrt{\pi}} \int_0^{\infty} dt \frac{e^{-[1-\Delta_{00}^{\text{MHF}}(k_x)]t}}{\sqrt{t}} \int_0^{\pi/2} d\varphi \frac{\exp(tk_x^2 \cos^2 \varphi / \{1 - [(e^{-\lambda^2 t} + \lambda^2 t - 1)/(\lambda^2 t)] \sin^2 \varphi\})}{\sqrt{1 - [(e^{-\lambda^2 t} + \lambda^2 t - 1)/(\lambda^2 t)] \sin^2 \varphi}}. \quad (21)$$

Performing now the 2D limit one obtains the polaron correction to the 2D energy-momentum relation  $\mathcal{E}_{2\text{D}}(k_x) = (1-\gamma^2)k_x^2$ :

$$\text{Re}\Sigma_{2\text{D}}^{\text{MHF}}[k_x, E_{2\text{D}}(k_x)] = -\frac{\alpha_p}{\sqrt{1-\Delta_{2\text{D}}^{\text{MHF}}(k_x)}} \mathbf{K}\left(\frac{k_x}{\sqrt{1-\Delta_{2\text{D}}^{\text{MHF}}(k_x)}}\right), \quad (22)$$

where  $\mathbf{K}(x)$  is the complete elliptical integral of the first kind. This result was first discussed by Peeters, Warmenbol, and Devreese,<sup>24</sup> who showed that  $|\text{Re}\Sigma_{2\text{D}}^{\text{MHF}}[k_x, E_{2\text{D}}(k_x)]| \rightarrow \infty$  if  $E_{2\text{D}}(k_x) - E_{2\text{D}}(0) \rightarrow 1$  and thus the 2D energy-momentum relation is pinned at this line. The TDA on-mass-shell result<sup>6</sup> is obtained with  $\Delta_{2\text{D}}^{\text{MHF}}(k_x)=0$  and is only valid for  $k_x \ll k_L \equiv \sqrt{2}m_e\omega_L/\hbar$ . In the case of vanishing wave-vector component  $k_x$ , from Eq. (22) and with  $\mathbf{K}(0)=\pi/2$  the well-known result

$$\text{Re}\Sigma_{2\text{D}}^{\text{MHF}}[0, E_{2\text{D}}(0)] = -\alpha_p \frac{\pi}{2} \quad (23)$$

follows. It is noticeable that the (modified) Hartree-Fock self-energy for the ground-state renormalization at  $k_x=0$  is identical to that in OMS, but differs from the TDA result, where

$$\text{Re}\Sigma_{2\text{D}}^{\text{TDA}}[0, E_{2\text{D}}(0)] = -\frac{\alpha_p \pi}{2} \frac{1}{\sqrt{1 - \text{Re}\Sigma_{2\text{D}}^{\text{TDA}}[0, E_{2\text{D}}(0)]}} \quad (24)$$

follows for  $B=0$  and  $\Omega=0$ .

In Figs. 2(a) and 2(b) the energy renormalizations of the ground-state level and of the first excited level,  $\text{Re}\Sigma_{00}$  and  $\text{Re}\Sigma_{11}$ , respectively, are depicted as functions of the magnetic field in the case of vanishing wave-vector component  $k_x=0$ . The calculations are done for MHFA, TDA, and OMS. The absolute values of  $\text{Re}\Sigma_{00}$  and  $\text{Re}\Sigma_{11}$ , i.e., the Q1D magnetopolaron binding energies, increase with in-

creasing magnetic field. Please note that  $\text{Re}\Sigma_{00}^{\text{MHF}} = \text{Re}\Sigma_{00}^{\text{OMS}}$  but  $\text{Re}\Sigma_{11}^{\text{MHF}} \neq \text{Re}\Sigma_{11}^{\text{OMS}}$ . For  $B=0$  we find for the matrix self-energies:  $\text{Re}\Sigma_{00}^{\text{MHF}} = -4.057$  meV,  $\text{Re}\Sigma_{00}^{\text{TDA}} = -3.850$  meV,  $\text{Re}\Sigma_{11}^{\text{MHF}} = -4.482$  meV,  $\text{Re}\Sigma_{11}^{\text{TDA}} = -4.206$  meV, and  $\text{Re}\Sigma_{11}^{\text{OMS}} = -4.516$  meV. These values are slightly enhanced compared to the strict 2D case ( $\text{Re}\Sigma_{2\text{D}}^{\text{HF}} = -3.978$  meV) and the 3D case ( $\text{Re}\Sigma_{3\text{D}}^{\text{HF}} = -2.532$  meV). It is seen that the OMS



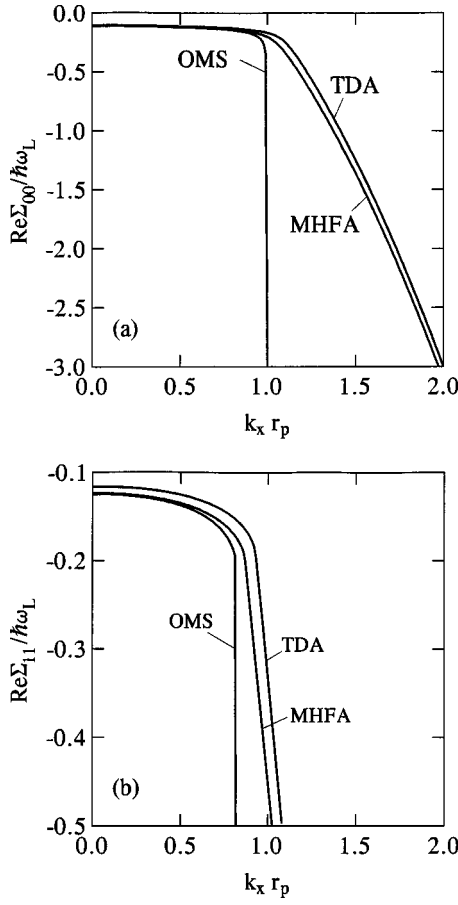


FIG. 5. The matrix self-energies  $\text{Re}\Sigma_{00}$  (a) and  $\text{Re}\Sigma_{11}$  (b) of the Q1D subbands  $\mathcal{E}_0$  and  $\mathcal{E}_1$ , respectively, for  $B=0$  as a function of wave-vector component  $k_x$  calculated in MHFA, TDA, and TDA on-mass shell (OMS).

result for  $\text{Re}\Sigma_{11}$  diverges negatively at the resonance of  $\mathcal{E}_{1;0q}$  with  $\mathcal{E}_{th}$ , i.e., slightly below  $\omega_c = \omega_L$ . It should be noted that the behavior of these self-energies on the magnetic field is very similar to that on the confining frequency.

The dependence of the first two renormalized and unrenormalized levels on the magnetic field is plotted in Fig. 3 for  $k_x=0$ . Here and in the following figures the energy-momentum relations are plotted as mentioned above without the Zeeman energy. If necessary one may add it with the result that two pictures arise, one shifted up and the other down by the Zeeman energy. The renormalized ground-state energy  $E_0$  is slightly below the unrenormalized ground-state energy  $\mathcal{E}_0$ , the first excited level  $E_1$  diverges negatively at the resonance, which appears in dependence on the confining frequency below of  $\omega_c = \omega_L$ , if calculated in TDA on-mass shell. Further,  $E_1$  approaches for large magnetic fields  $\mathcal{E}_0 + 1$  if calculated in TDA [see Fig. 3(b)], i.e., the pinning appears at the wrong energy inside the renormalized phonon continuum. Only the MHFA gives the correct pinning of  $E_1$  for large magnetic fields at the threshold of the renormalized one-phonon continuum [see Fig. 3(a)], i.e., at the correct ground state plus one LO phonon:  $E_0 + 1$ . Because the behavior of the renormalized energy levels in dependence on the magnetic field is very similar to that on the lateral confining potential of the QWW, we come to the conclusion that

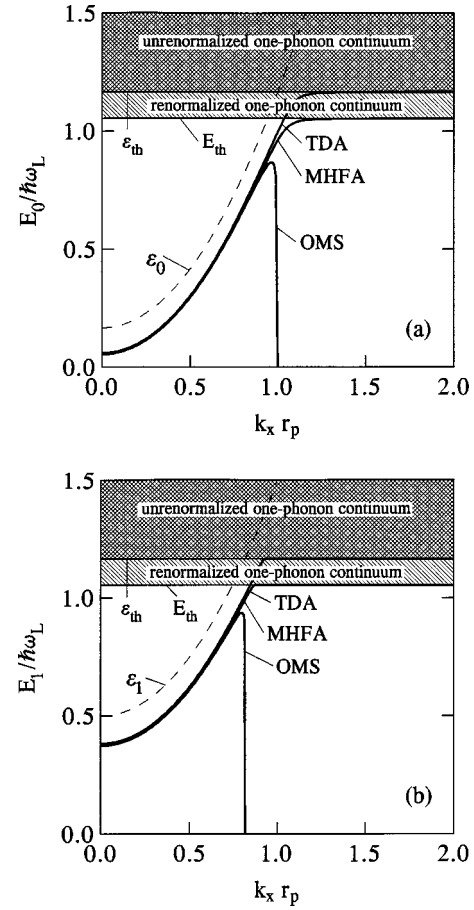


FIG. 6. The energy-momentum relation of the lowest level  $E_0(k_x)$  (a) and of first excited level  $E_1(k_x)$  (b) calculated in MHFA, TDA, and OMS for  $B=0$  (heavy solid lines). The corresponding unperturbed dispersion relations  $\mathcal{E}_0(k_x)$  and  $\mathcal{E}_1(k_x)$  are plotted by the dashed lines. The hatched areas show the renormalized and the unrenormalized phonon continuum.

even at  $B=0$  and  $k_x=0$ , TDA and TDA on-mass shell are useful only for QWW's with weak confinement potential, i.e., if  $\Omega \ll \omega_L$ .

The lowest subband energy  $E_0(k_x; B)$  including the polaronic corrections in MHFA is plotted in Fig. 4 as a function of the magnetic field for different (zero-phonon) magnetopolaron momenta  $\hbar k_x^{\text{pol}} = \hbar k_x$ . It is seen from Fig. 4(a) that for vanishing magnetopolaron momentum the energy  $E_0(k_x=0; B)$  increases with increasing magnetic field. For a finite magnetopolaron momentum the energy  $E_0(k_x \neq 0; B)$  shows a minimum at  $B \neq 0$  [see Fig. 4(b)]. This minimum is caused by the magnetic-field dependence of the effective mass  $\tilde{m}_e$ . With increasing magnetic field the effective mass  $\tilde{m}_e$  increases and thus the kinetic energy decreases while the confining energy  $\hbar\tilde{\omega}_c$  increases. In Figs. 4(c) and 4(d) it is assumed that the ground-state plus kinetic energy is so large that the noninteracting single-particle energy  $\mathcal{E}_0(k_x \neq 0; B=0)$  lies within the phonon continuum. The electron-phonon interaction will result in a shift of the zero-phonon magnetopolaron quasiparticle energy below the boundary of the one-phonon continuum. This is valid for all coupling strengths  $\alpha_p$  and thus is a special feature of the resonance of a discrete state with a continuum of states.

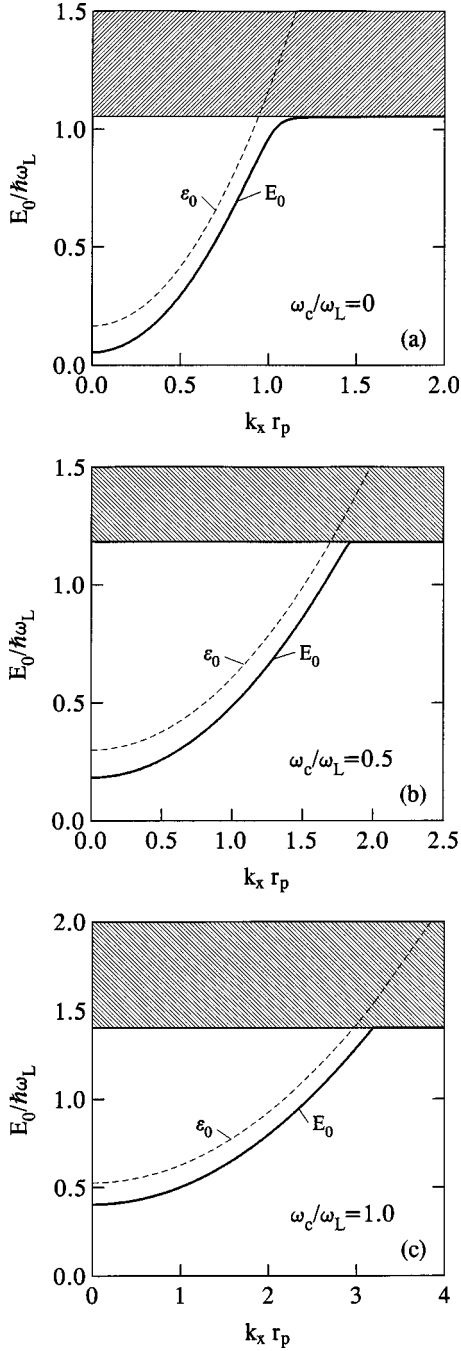


FIG. 7. Energy-momentum relation for Q1D magnetopolarons in the lowest subband  $E_0(k_x; B)$  (heavy solid line) calculated in MHFA for different magnetic field strengths: (a)  $\omega_c/\omega_L=0$ , (b)  $\omega_c/\omega_L=0.5$ , and (c)  $\omega_c/\omega_L=1.0$ . The corresponding unperturbed dispersion relation  $\mathcal{E}_0(k_x; B)$  is plotted by the dashed line. The renormalized phonon continuum is shown by the hatched area.

In Figs. 5(a) and 5(b) we show the wave-vector dependence of the self-energies  $\text{Re}\Sigma_{00}$  and  $\text{Re}\Sigma_{11}$  for  $B=0$  calculated with MHFA, TDA, and OMS. It is seen that with increasing momentum the absolute value of the self-energy increases, and  $\text{Re}\Sigma_{00}^{\text{OMS}}$  and  $\text{Re}\Sigma_{11}^{\text{OMS}}$  diverge negatively at  $k_x = k_L^{(0)} = 1$  and  $k_x = k_L^{(1)} = \sqrt{1 - \Omega/\omega_L}$ , respectively.

The resulting energy-momentum relations of the Q1D polarons in subbands  $N=0$  and  $N=1$  are plotted in Figs. 6(a) and 6(b) for  $B=0$ . It is seen that the TDA on-mass-shell

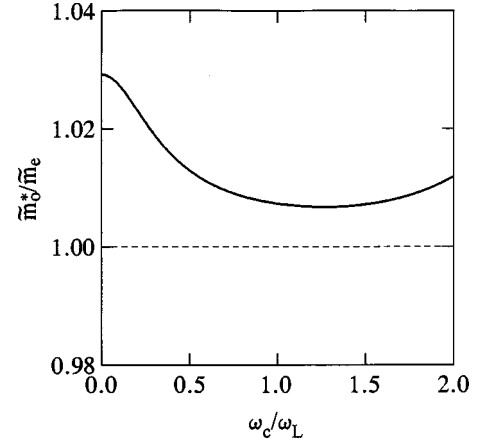


FIG. 8. Magnetopolaron effective mass of the lowest subband  $\tilde{m}_0^*$  in dependence on the magnetic field calculated in MHFA (heavy solid line). The magnetic-field-dependent noninteracting effective mass  $\tilde{m}_e$  is plotted by the dashed line.

dispersion curves diverge negatively at  $k_x = k^{(N)}$ , the TDA dispersion curves bend over and become pinned at the threshold of the unrenormalized one-phonon continuum,  $\mathcal{E}_{\text{th}} = \mathcal{E}_0(0) + 1$ , and only the MHFA dispersion curves show the correct pinning at the threshold of the renormalized one-phonon continuum  $E_{\text{th}} = E_0(0) + 1$ .

The energy-momentum relation of the Q1D magnetopolaron  $E_0 = E_0(k_x; B)$  calculated in MHFA is plotted in Fig. 7 for different strengths of the magnetic field. It can be seen from these figures that the magnetopolaron dispersion curve bends over at the threshold  $E_{\text{th}} = E_0(0) + 1$  of the one-phonon continuum. The bend-over region shifts to higher magnetopolaron momenta with increasing magnetic field [see Figs. 7(a) to 7(c)]. It should be noted that at  $T=0$  a Q1D magnetopolaron with energy-momentum relation as plotted in Figs. 4 and 7 cannot emit a real LO phonon, because of the always finite energy difference between  $E_0(k_x; B)$  and  $E_{\text{th}}$ . In real systems, however, the energy levels are broadened due to impurity scattering processes. Then, it could be possible that the magnetopolaron emits a real LO phonon if its energy is large enough. After emitting this LO phonon the magnetopolaron relaxes to the subband bottom. This process should result in an oscillation of the electron group velocity if an electric field is applied along the wire. In the high-field magnetotransport, which is essentially ballistic in GaAs-Ga<sub>1-x</sub>Al<sub>x</sub>As QWW's, these electron velocity oscillations should be measurable.

The magnetopolaron effective mass  $\tilde{m}_0^*$  of the lowest subband  $E_0(k_x)$  is plotted in Fig. 8. It is calculated from Eq. (11), which can be written in diagonal approximation in the form

$$\frac{\tilde{m}_N^*}{\tilde{m}_e} = \lim_{k_x \rightarrow 0} \left\{ 1 + \frac{1}{1 - \gamma^2} \frac{1}{2k_x} \frac{d}{dk_x} \text{Re}\Sigma_{NN}^{\text{MHF}}[k_x, E_N(k_x)] \right\}^{-1}. \quad (25)$$

The effective mass quotient  $\tilde{m}_0^*/\tilde{m}_e$  decreases for smaller magnetic fields with increasing magnetic field because in this range  $1 - \gamma^2$  tends to zero more slowly than  $(1/2k_x)(d/dk_x)\text{Re}\Sigma_{00}^{\text{MHF}}|_{k_x \rightarrow 0}$ . For  $B=0$  we have  $\tilde{m}_0^*/\tilde{m}_e = m_0^*/m_e$

=1.029, a value somewhat larger than for the strict 2D interacting electron-phonon system ( $m_{2D}^*/m_e=1.028$ ) and for the 3D counterpart ( $m_{3D}^*/m_e=1.012$ ) For larger magnetic fields the mass quotient increases with increasing magnetic field. It should be noted that this mass is quite different from the magnetopolaron cyclotron mass  $m_c^*/m_e = \hbar\omega_c/\sqrt{(E_N-E_{N-1})^2-(\hbar\Omega)^2}$ , discussed in detail in Ref. 17.

In summary, we have developed a theory based on Feynman-Dyson perturbation theory that allows quite generally the calculation of the quasiparticle properties in the subband space of lower-dimensional semiconductor nanostructures. Using this theory the quasiparticle properties of Q1D magnetopolarons in QWW's are investigated in the framework of a modified Hartree-Fock approximation. It is shown that compared with the old-fashioned perturbation theories

only the Green's-function method allows one to consider all different intersubband scattering processes. The results presented here for the Q1D magnetopolaron become identical to the modified improved Wigner-Brillouin perturbation theory<sup>16,17</sup> if two diagonal approximations for the intersubband processes are performed. It is shown that the obtained energy-momentum relations show the correct bend over and pinning at the threshold of the one-phonon continuum. TDA and TDA on-mass shell fail for the calculation of the renormalized subband energies in QWW's with strong lateral confinement potentials even at  $B=0$  and  $k_x=0$ . In this case only the MHFA gives correct results for the renormalized subband energies. Thus, the modified Hartree-Fock approximation is the simplest procedure to obtain in a suitable way correct results for the magnetopolaronic quasiparticle properties for all  $B$ ,  $k_x$ , and confining potentials of quantum-well wires.

- 
- <sup>1</sup> *Polarons and Excitons*, edited by C. Kuper and G. Whitfield (Oliver & Boyd, Edinburgh, 1963).
- <sup>2</sup> *Polarons in Ionic Crystals and polar semiconductors*, edited by J.T. Devreese (North-Holland, Amsterdam, 1972).
- <sup>3</sup> S. Das Sarma and A. Madhukar, Phys. Rev. B **22**, 2823 (1980).
- <sup>4</sup> D. Larsen, Phys. Rev. B **30**, 4595 (1984).
- <sup>5</sup> R. Lassnig and W. Zawadzki, Surf. Sci. **142**, 388 (1984).
- <sup>6</sup> S. Das Sarma and D. Mason, Ann. Phys. (N.Y.) **163**, 78 (1985).
- <sup>7</sup> F.M. Peeters and J.T. Devreese, Phys. Rev. B **31**, 3689 (1985).
- <sup>8</sup> R. Haupt and L. Wendler, Ann. Phys. (N.Y.) **233**, 214 (1994).
- <sup>9</sup> R. Haupt and L. Wendler, Z. Phys. B **94**, 49 (1994).
- <sup>10</sup> R. Haupt and L. Wendler, Semicond. Sci. Technol. **9**, 803 (1994).
- <sup>11</sup> R. Haupt and L. Wendler, Solid State Commun. **89**, 741 (1994).
- <sup>12</sup> L. Wendler, A.V. Chaplik, R. Haupt, and O. Hipólito, J. Phys.: Condens. Matter **5**, 8031 (1993).
- <sup>13</sup> M.H. Degani and O. Hipólito, Phys. Rev. B **35**, 9345 (1987).
- <sup>14</sup> M.H. Degani and O. Hipólito, Solid State Commun. **65**, 1185 (1988).
- <sup>15</sup> H.Y. Zhou, K.-D. Zhu, and S.-W. Gu, J. Phys.: Condens. Matter **4**, 4613 (1992).
- <sup>16</sup> L. Wendler and R. Kügler, J. Phys.: Condens. Matter **6**, 7857 (1994).
- <sup>17</sup> L. Wendler, A.V. Chaplik, R. Haupt, and O. Hipólito, J. Phys.: Condens. Matter **5**, 4817 (1993).
- <sup>18</sup> L. Wendler and R. Pechstedt, Phys. Status Solidi B **138**, 197 (1986).
- <sup>19</sup> In general the Green's function can be separated in two parts, one part consists of the single isolated poles and the second part, called the incoherent part  $g_{NN';\alpha}^{\text{inc}}$ , results from the background and is finite in the region where the poles exist. The part describing the poles is thus a meromorphic, or more specific a rational function, if the number of poles is finite. A meromorphic function  $f(z) = G_{NN';\alpha}^R(k_x, z) - g_{NN';\alpha}^{\text{inc}}(k_x, z)$  with only single poles at  $z = z_\nu$  can be represented as  $f(z) = \sum_\nu \text{Res}_{z=z_\nu} f(z)/(z - z_\nu) + g(z)$ , where  $g(z)$  is an entire function. The “ $\approx$ ” sign in Eq. (5) results from the fact that  $g_{NN';\alpha}^{\text{inc}}$  and  $g$  are neglected in this representation.
- <sup>20</sup> L. Wendler, R. Haupt, and R. Pechstedt, Phys. Rev. B **43**, 14 669 (1991).
- <sup>21</sup> L. Wendler and V.G. Grigoryan, Phys. Rev. B **54**, 8652 (1996).
- <sup>22</sup> L. Wendler, R. Kügler, and R. Haupt, in *Proceedings of the 11th International Conference on High Magnetic Fields in the Physics of Semiconductors*, edited by D. Heiman (World Scientific Publishing, Singapore, 1995), p. 520.
- <sup>23</sup> G. Lindemann, R. Lassnig, W. Seidenbusch, and E. Gornik, Phys. Rev. B **28**, 4693 (1983).
- <sup>24</sup> F.M. Peeters, P. Warmenbol, and J.T. Devreese, Europhys. Lett. **3**, 1219 (1987).